

# Quantitative Prediction of Stress Corrosion Crack Propagation Rate of Small Crack in Alloy 600 for Nuclear Pressure Vessels

Fang Xiurong, Yang Jinhui, Shao Yanru, Ou Xue

*Xi'an University of Science & Technology, Xi'an 710054, China*

**Abstract:** Stress corrosion crack (SCC) of small crack has an important effect on the whole-life attenuation process of critical structures in nuclear power plants (NPPs). By combining the film slip-dissolution/oxidation model with the elastic-plastic finite element method (EPFEM), the SCC propagation rate for small crack in reactor pressure vessels (RPVs) of NPPs was quantitatively predicted. According to the crack tip mechanical field analysis, the crack tip strain rate was determined to control the initiation and propagation of small cracks, and it was approximately calculated by the variation of plastic strain ( $d\varepsilon_p/da$ ) at a characteristic distance  $r_0$  to the growing small crack tip. Two methods of dynamic crack propagation and quasi-static crack propagation based on EPFEM were proposed to calculate the variation of plastic strain ( $d\varepsilon_p/da$ ). The contrast of the two calculation methods and the sensitivity analysis of variation of plastic strain with the crack length were carried out. The results show that there is a slight difference between the two methods, and the plastic strain variation is more sensitive to the crack propagation of small crack than to the long crack. The SCC propagation rate of small cracks is larger than that of long cracks, and it is significantly influenced by the characteristic distance  $r_0$ . As it is difficult to determine the value of characteristic distance  $r_0$  finally, it is suggested to be determined by combining experimental SCC data with finite element simulation of the single-edge crack panel specimens under the same environmental and material conditions.

**Key words:** alloy 600; stress corrosion crack; quantitative prediction; crack tip strain; elastic plastic finite element method

According to the Power Reactor Information System (PRIS) maintained by the International Atom Energy Agency (IAEA), many nuclear power plants (NPPs) have been operated for over 30 years, with service ages almost reaching the design life of 40 years<sup>[1]</sup>. Due to the high cost of new nuclear power plants, it is an important choice for many countries to extend the life of NPPs. However, safety is still the primary factor when considering the life extension of NPPs. As the structural materials used in the NPPs continue to suffer from the high temperature, high pressure, nuclear irradiation and corrosion environment, the degeneration of material is serious<sup>[2]</sup>, so it is important to acquire how the materials degenerate and verify the actual state of structures in order to assess their residual life. Stress corrosion crack (SCC) is an important form of

material degradation, and scholars have concluded many SCC mechanisms and quantitative prediction models<sup>[3,4]</sup>. Researchers have shown that for high strength alloy materials, the service life of components is mainly controlled by the initiation and the propagation behavior of small fatigue cracks, and the mechanical behavior of small crack is obviously discriminated with long crack<sup>[5]</sup>; thus the prediction of crack propagation rates for small cracks is one of the key issues when predicting the residual life of structures used in NPPs.

As it is difficult to obtain sufficient SCC experimental data of small cracks at high temperature, the numerical simulation method is adopted in this paper to verify the SCC crack tip mechanical field and crack propagation rates of small cracks on the surface of alloy 600, which is used to produce reactor

Received date: August 19, 2018

Foundation item: National Natural Science Foundation of China (51775427)

Corresponding author: Fang Xiurong, Ph. D., Associate Professor, School of Mechanical Engineering, Xi'an University of Science and Technology, Xi'an 710054, P. R. China, Tel: 0086-29-85583159, E-mail: fangxr098@163.com

Copyright © 2019, Northwest Institute for Nonferrous Metal Research. Published by Science Press. All rights reserved.

pressure vessels (RPVs) in AP1000 NPPs. The pressure vessel services at a specific temperature in nuclear power plants (NPPs). The performance of its structural materials is different from that at room temperature. Stress corrosion crack (SCC) research is mainly focused on the crack initiation and crack propagation of material, and the characteristic at the crack tip of material is analyzed on the basis of the mechanical field at the crack tip of certain material. Therefore, in this paper, the mechanical field of the crack tip was analyzed by comparing the mechanical properties of alloy 600 at normal temperature and 340 °C boiling water reactor.

### 1 SCC Quantitative Prediction Model of Small Crack

The Ford-Andresen model<sup>[6,7]</sup> are widely used to predict the crack propagation rate of structure materials used in high temperature water environments of NPPs. The model combines the electrochemical environment, material and mechanical factors at the crack tip region into a formula, and the crack growth rate is expressed as:

$$\frac{da}{dt} = \kappa_a (\dot{\epsilon}_{ct})^m \quad (1)$$

where  $da/dt$  is the SCC rate,  $\dot{\epsilon}_{ct}$  is the crack tip strain rate, and  $m$  is the current decay curve index;  $\kappa_a$  is the crack tip oxidation rate constant, which is determined by the electrochemical environment and the material in the vicinity of the crack tip, and it is defined as:

$$\kappa_a = \frac{M}{Z\rho F} \cdot \frac{i_0}{1-m} \cdot \left(\frac{t_0}{\epsilon_f}\right)^m \quad (2)$$

where  $M$  is the atomic mass of the metal,  $\rho$  is the density of the metal,  $Z$  is the charge due to the oxidation process,  $F$  is Faraday's constant,  $i_0$  is exposed surface oxidation current density,  $t_0$  is the initial time of current decay, and  $\epsilon_f$  is the fracture strain of oxide film on the crack tip.

In Eq.(1), the crack tip strain rate  $\dot{\epsilon}_{ct}$ , which controls the passive film rupture frequency and determines the average dissolution current, plays a key role in determining the crack propagation rate. However, it is difficult to obtain the strain rate of crack tip directly in practical applications. By adopting the strain redistribution and the strain gradient of a steady growing crack front<sup>[8]</sup>, the FRI model developed by Satoh et al to predict the SCC propagation rate was expressed as<sup>[9]</sup>:

$$\frac{da}{dt} = \kappa_a \left\{ \beta \frac{\sigma_y}{E} \frac{n}{n-1} \left( 2 \frac{\dot{K}}{K} + \frac{\dot{a}}{r_0} \right) \left[ \ln \left( \frac{R_p}{r} \right)^{\frac{1}{n-1}} \right] \right\}^m \quad (3)$$

where  $\beta$  is dimensionless constant,  $\sigma_y$  is yield strength,  $E$  is elastic modulus,  $r$  is distance to the crack tip,  $K$  is stress intensity factor,  $n$  is strain hardening index,  $R_p$  is plastic zone size, and  $\lambda$  is constraint factor.

However, many parameters in Eq.(3) are difficult to acquire, so it is still difficult to obtain an accurate crack propagation

rate. The mechanical field at small crack tip shows that the characteristic of small crack can be described by strain, and the strain gradient change of small crack is bigger than that of long crack. Thus it was proposed that the crack tip strain  $\epsilon_{ct}$  can be replaced by the tensile plastic strain  $\epsilon_p$  at a characteristic distance  $r_0$  to the front of the tip<sup>[10]</sup>:

$$\epsilon_{ct} = \epsilon_p \Big|_{r=r_0} \quad (4)$$

where  $\epsilon_p$  is the equivalent plastic strain at the characteristic distance of  $r_0$  in front of the growth tip. Thus,

$$\frac{d\epsilon_{ct}}{dt} = \frac{d\epsilon_p}{dt} = \left( \frac{d\epsilon_p}{da} \right) \cdot \left( \frac{da}{dt} \right) \quad (5)$$

where  $d\epsilon_p/da$  is the variation in tensile plastic strain with crack growth at the characteristic distance  $r_0$  in front of the crack tip.

Substituting Eq.(5) into Eq.(1), the SCC propagation rate can be written as,

$$\frac{da}{dt} = \kappa_a' \left( \frac{d\epsilon_p}{da} \right)^{1/(1-m)} \quad (6)$$

where,

$$\kappa_a' = \kappa_a^{1/(1-m)} \quad (7)$$

Using the elastic-plastic finite element method (EPFEM), the  $d\epsilon_p/da$  at the characteristic distance  $r_0$  in front of the crack tip can be approximately calculated by two methods, and the basic calculation conception is depicted in Fig.1.

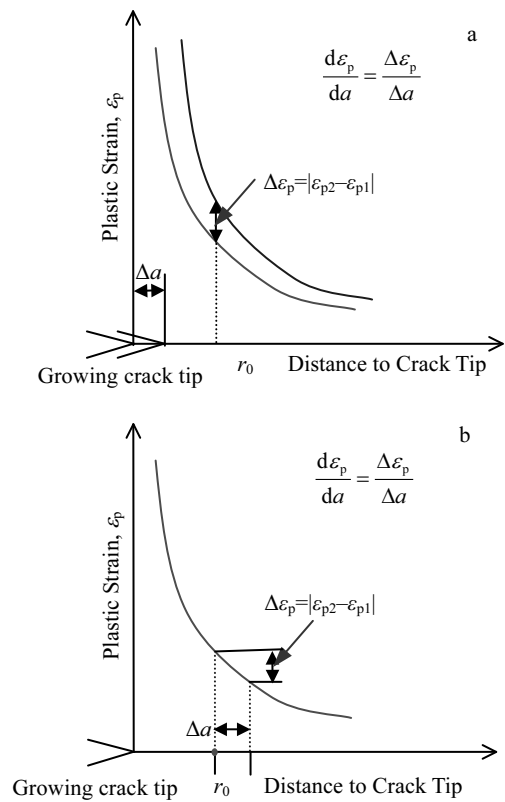


Fig.1 Relationship between  $\Delta a$  and  $\Delta \epsilon_p$  in numerical simulation: (a) dynamic crack propagation method and (b) quasi-static propagation method

As shown in Fig.1a, the initial crack length is  $a$ , and the plastic strain at the characteristic distance  $r_0$  in front of the crack tip is  $\varepsilon_{p1}$ . When the cracks propagate  $\Delta a$ , the position to calculate the plastic strain does not change, and the plastic strain changes to  $\varepsilon_{p2}$ . The plastic strains of  $\varepsilon_{p1}$  and  $\varepsilon_{p2}$  are obtained by finite element analysis<sup>[11]</sup>. And accordingly,  $d\varepsilon_p/da$  can be obtained by the following expression:

$$\frac{d\varepsilon_p}{da} \approx \frac{\Delta\varepsilon_p}{\Delta a} = \frac{\varepsilon_{p2}|_{r=r_0+\Delta a} - \varepsilon_{p1}|_{r=r_0}}{\Delta a} \quad (8)$$

where  $\varepsilon_{p1}$  and  $\varepsilon_{p2}$  are the plastic strain at the characteristic distance  $r_0$  in front of the initial crack tip, with a crack propagation of  $\Delta a$ .

As the plastic strains  $\varepsilon_{p1}$  and  $\varepsilon_{p2}$  are calculated at the same initial position with crack length of  $a$ , at the propagated stage where crack length equals to  $a+\Delta a$ , the method for calculating  $d\varepsilon_p/da$  by Eq.(8) is called as dynamic crack propagation method. By this method, at least two calculation models or steps are needed for calculating.

The other method for calculating  $d\varepsilon_p/da$  is shown in Fig.1b. It is assumed that the plastic strain is always acquired at the characteristic distance  $r_0$  in front of the crack tip, which means that when the crack propagates  $\Delta a$ , the characteristic distance propagates  $\Delta a$  to  $\Delta a+r_0$ , simultaneously. And the  $d\varepsilon_p/da$  is calculated as,

$$\frac{d\varepsilon_p}{da} \approx \frac{\Delta\varepsilon_p}{\Delta a} = \frac{\varepsilon_{p2}|_{r=r_0+\Delta a} - \varepsilon_{p1}|_{r=r_0}}{\Delta a} \quad (9)$$

If  $\Delta a$  is small enough, the  $d\varepsilon_p/da$  has the physical meaning

of plastic strain gradient at the characteristic distance  $r_0$  in front of the crack tip. By this method, the  $d\varepsilon_p/da$  can be calculated by one simulation model or step without the propagation of crack. Thus it is called quasi-static crack propagation method using Eq.(9).

Substituting Eq.(8) or Eq.(9) into Eq.(6), the growth rate of the crack can be obtained.

## 2 Calculation Model

### 2.1 Geometric model and mesh model

A 2D-plate (the single-edge crack panel) specimen with a crack is adopted in this simulation<sup>[12]</sup>. As shown in Fig.2, the specimen length and width are 50 mm and 20 mm, respectively, and  $a$  represents the initial crack length. In order to highlight the anomalous mechanical behavior of small crack tip, the crack length  $a$  is selected from 0.2 mm to 2 mm arbitrarily.

The specimen is meshed with CPE8 element, and the crack tip region is refined to get more detailed and accurate data of crack tip's mechanical parameters.

### 2.2 Material model

Experiments show that the fracture properties of alloy 600 exhibit stronger ductility at high temperature<sup>[13]</sup>. Therefore, the Ramberg-Osgood relationship is adopted to represent its power hardening characteristic. The mechanical properties of alloy 600 at normal temperature and 340 °C boiling water reactor are shown in Table 1<sup>[14]</sup>.

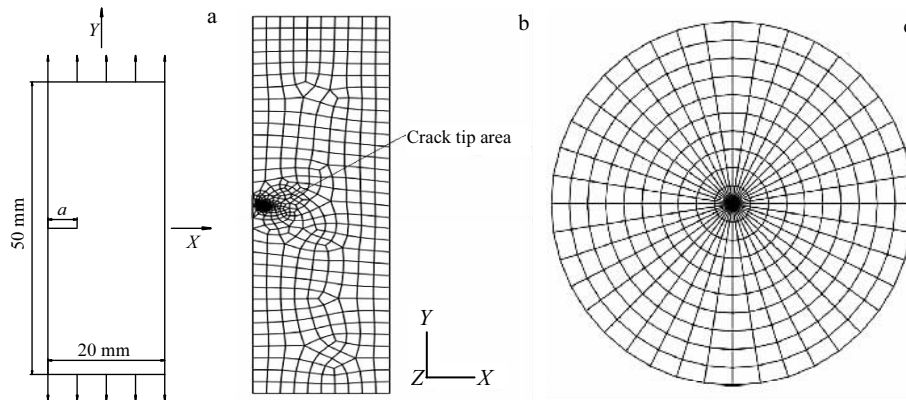


Fig.2 Geometric model (a), global mesh model (b), and refined mesh of crack tip (c)

Table 1 Mechanical properties of alloy 600<sup>[14]</sup>

Parameter	Normal temperature	340 °C
Young's modulus, $E$ /GPa	214	189.5
Poisson's ratio, $\nu$	0.324	0.286
Yield strength, $\sigma_{ys}$ /MPa	550	436
Hardening exponent, $n$	8.193	6.495
Yield offset, $\alpha$	3.879	3.075

The main purpose of this study is to evaluate the effect of the mechanical factor on SCC behavior. The oxidation rate constant  $\kappa_a'$  was set to  $7.478 \times 10^{-7}$ , and the index of the current decay curve  $m$  was set to 0.5<sup>[15]</sup>.

### 2.3 Load condition

The SCC growth is related to the crack tip stress intensity factor  $K_I$ . Thus a constant  $K_I$  was used for different crack lengths to ensure the same load condition<sup>[16]</sup>. It is known that

the designed pressure of AP1000 reactor pressure vessel, which has a diameter of about 5 m and a thickness exceeding 20 cm, is up to 17.23 MPa, generally operated under the pressure of 15.5 MPa<sup>[17,18]</sup>. According to the stress theory of pressure vessel design, combined with the calculation formula of fracture mechanics, the crack tip stress intensity factor  $K_I$  equals to 7 MPa·m<sup>1/2</sup> for a small crack located at the surface of RPVs<sup>[19]</sup>. As shown in Fig.2, uniform tensile stress is applied on the top and bottom surfaces of the specimen to ensure the crack tip stress intensity factor, and the tensile stress is calculated as:

$$\sigma = K_I / \sqrt{\pi a} \quad (10)$$

where  $\sigma$  is the tensile stress applied;  $K_I$  is the crack tip intensity factor, which always equals to 7 MPa·m<sup>1/2</sup> in this study;  $a$  is the crack length.

### 3 Result and Discussion

#### 3.1 Mechanical characteristic of small crack tip

The Von Mises stress in front of crack tip is shown in Fig.3. It can be seen that whether the crack length is equal to 0.2 mm or 2 mm, the Mises stress distribution curves almost coincide with each other in normal temperature and high temperature environments, which indicates that the mechanical property change caused by the service temperature has few effects on the Mises stress in front of the crack tip.

Strain is another important parameter to characterize the crack tip fracture. As shown in Fig.4, when the service temperature changes from normal temperature to 340 °C, the

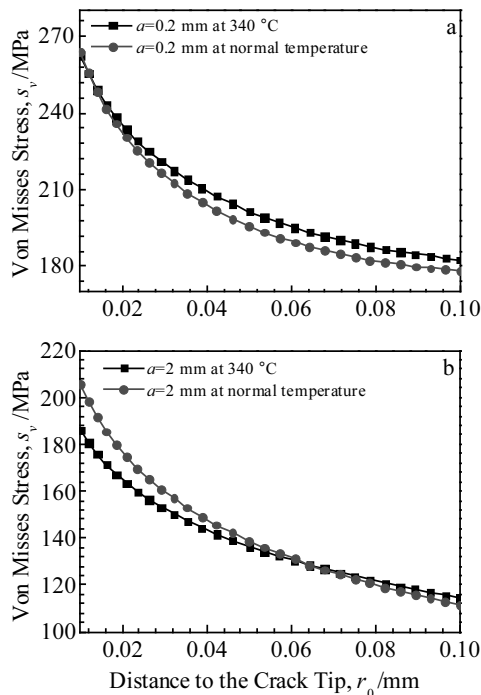


Fig.3 Mises stress distribution in front of small crack tip: (a) crack length  $a=0.2$  mm and (b) crack length  $a=2$  mm

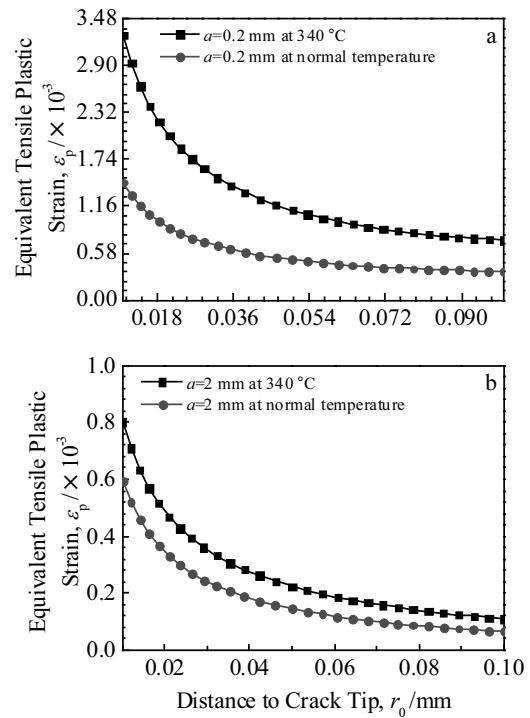


Fig.4 Equivalent plastic strain distribution in front of small crack tip: (a) crack length  $a=0.2$  mm and (b) crack length  $a=2$  mm

equivalent plastic strain in front of small crack tip increases significantly, especially the small crack with 0.2 mm in length. Thus, it can be concluded that strong strain strengthening occurs in crack tip regions in high temperature water environments<sup>[20]</sup>.

The contrast of crack tip plastic zone at normal temperature and 340 °C is shown in Fig.5, in which contours 1 and 2 are the crack tip plastic zone boundaries under the same load condition. It can be seen that the plastic zone at 340 °C is bigger than at normal temperature for the same crack length, and the plastic zone of small crack is bigger than that of long crack at the same service temperature. With a constant load, the larger the plastic zone, the greater the crack growth driving force. Thus, the crack tip plastic zone size can be considered as a major factor influencing the crack growth rate of small crack<sup>[21]</sup>, whose size can also be represented by the characteristic distance  $r_0$  in front of the crack tip.

#### 3.2 Variation of plastic strain $d\varepsilon_p/da$ in front of a growing small crack tip

As shown in Fig.6, the plastic strain  $d\varepsilon_p/da$  at the characteristic distance  $r_0$  in front of the crack tip with different crack lengths is calculated by the dynamic crack propagation method and quasi-static crack propagation method, according to Eq.(8) and Eq.(9), respectively. It can be seen that for both calculation methods, the variation in plastic strain with crack growth ( $d\varepsilon_p/da$ ) decreases with the increase of characteristic distance  $r_0$ , and increases with the increase of crack length.

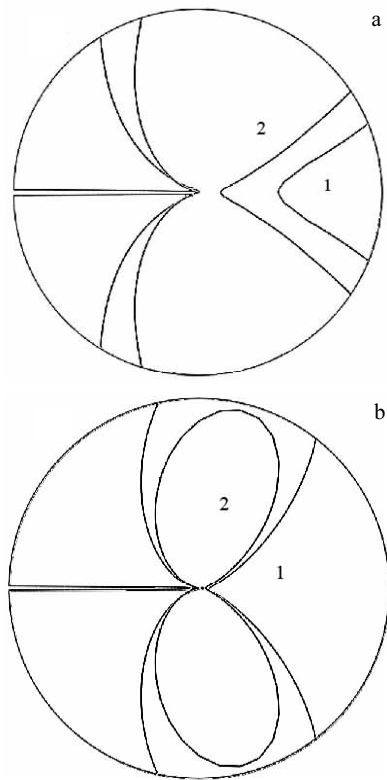


Fig.5 Contrast of crack tip plastic zone at normal temperature (contour 2) and 340 °C (contour 1): (a) crack length  $a=0.2$  mm and (b) crack length  $a=2$  mm

Defining  $\gamma$  as:

$$\gamma = \frac{d\varepsilon_p/da|_{\text{static}}}{d\varepsilon_p/da|_{\text{dynamic}}} \quad (11)$$

where  $\gamma$  is the specific value of plastic strain variation with crack growth calculated by the quasi-static crack propagation method ( $d\varepsilon_p/da|_{\text{static}}$ ) and dynamic crack propagation method ( $d\varepsilon_p/da|_{\text{dynamic}}$ ), and the contrast of plastic strain variation with crack growth calculated by the two methods is shown in Fig.7. It can be seen that the average specific value decreases slightly from 1.035 to about 1.030 when crack propagates from 0.3 mm to 2 mm, indicating that the difference between the two methods decreases with the increase of crack length. As the specific values are always above 1, the plastic strain variation with crack growth calculated by quasi-static crack propagation method is larger than that calculated by dynamic crack propagation method. However, the difference is very tiny because the specific values are close to 1. The small standard deviation at a certain crack length in Fig.7 indicates that the difference between  $d\varepsilon_p/da|_{\text{static}}$  and  $d\varepsilon_p/da|_{\text{dynamic}}$  at a certain crack length is not affected by the characteristic distance  $r_0$ .

Defining sensitivity coefficient  $\chi$  as:

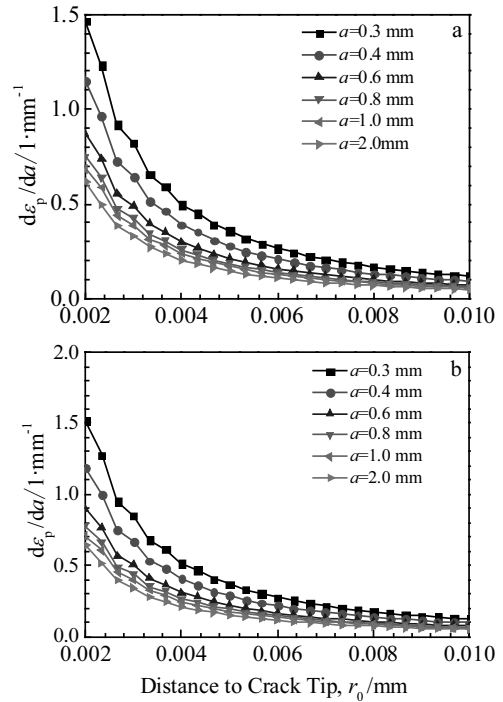


Fig.6 Variation in plastic strain with crack growth in front of crack tip calculated by dynamic crack propagation method (a) and quasi-static crack propagation method (b)

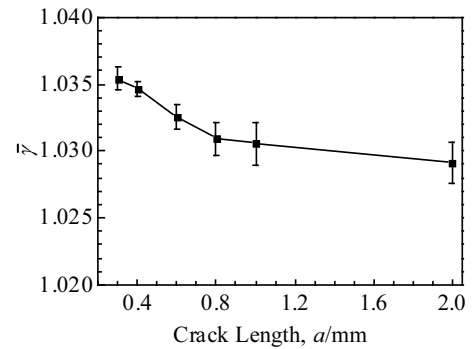


Fig.7 Contrast of plastic strain variation with crack growth calculation by quasi-static crack propagation method and dynamic crack propagation method

$$\chi = \frac{(d\varepsilon_p/da|_{a_{i+1}} - d\varepsilon_p/da|_{a_i}) / (d\varepsilon_p/da|_{a_i})}{(a_{i+1} - a_i) / a_i} \quad (12)$$

where sensitivity coefficient  $\chi$  denotes sensitivity of plastic strain variation with crack growth to crack length change.  $d\varepsilon_p/da|_{a_{i+1}}$  and  $d\varepsilon_p/da|_{a_i}$  are plastic strain variation with crack growth at crack lengths  $a_{i+1}$  and  $a_i$ , respectively.

The sensitivity coefficients  $\chi$  shown in Fig.8 are all negative, which indicates that the plastic strain variation decreases with

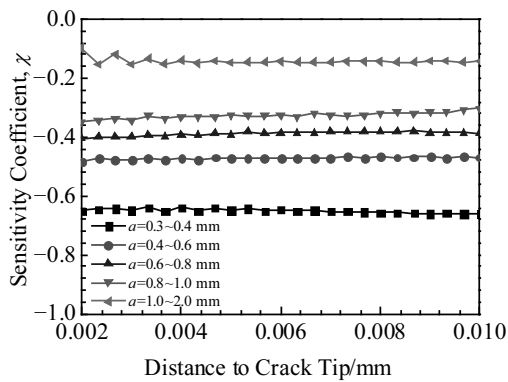


Fig.8 Sensitivity of plastic strain variation with crack growth to crack length change

the crack propagation. As the absolute values of sensitivity coefficient are smaller than 1, the change percentage of plastic strain variation is smaller than that of crack length, denoting a small influence of crack length change on plastic strain variation. However, the plastic strain variation is more sensitive to small crack propagation than to long crack, which can be supported by the decrease of absolute values of sensitivity coefficient with the increase of crack length. An obvious feature of the sensitivity coefficient curves shown in Fig.8 is that the curves are almost parallel to the  $x$ -axis, denoting that the sensitivity coefficient approximately equals to each other in front of crack tip with a certain crack length. The average sensitivity coefficient for certain crack length is calculated, as illustrated in Fig.9. It can be seen that in the range of 0.3~0.4 mm, with 33% change of crack length, plastic strain variation decreased to 65%, while it only decreased to 14% with 100% change of crack length in the range of 1~2 mm.

### 3.3 Estimation of SCC propagation rates for small crack

Substituting  $d\varepsilon_p/da$  into the basic formula Eq.(6), the SCC propagation rates for small crack are shown in Fig.10. It can be seen that the SCC propagation rates are obviously influenced

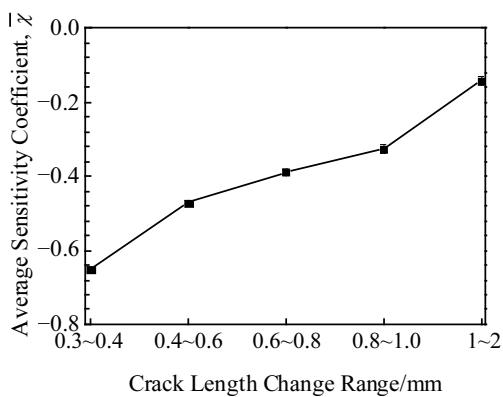


Fig.9 Average sensitivity coefficient for different crack length change ranges

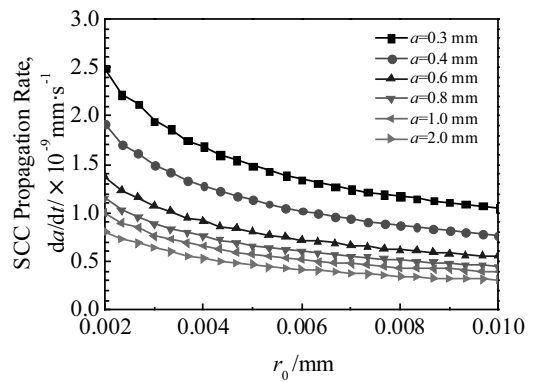


Fig.10 SCC propagation rates in front of crack tip

by the characteristic distance to the crack tip,  $r_0$ . For instance, if the crack length equals to 3 mm, the calculated SCC propagation rate is  $2.50 \times 10^{-7}$  mm/s with characteristic distance  $r_0=0.002$  mm, while the calculated SCC propagation rate decreases to about  $1.05 \times 10^{-7}$  mm/s with a characteristic distance  $r_0=0.002$  mm. The SCC propagation rate gradient in front of crack tip was calculated, as shown in Fig.11. It can be seen that the effects of characteristic distance on SCC propagation are significant for small characteristic distance  $r_0$ , and the effect decreases with the increase of  $r_0$ .

As the SCC propagation rate varies with different characteristic distances  $r_0$ , it is very important to determine the value of  $r_0$ . Unfortunately, the meaning of characteristic distance  $r_0$  is still unclear, so its value is difficult to determine finally. It is suggested that  $r_0$  can be determined by combining experimental SCC data with finite element simulation of the single-edge crack panel specimens under the same environment and material conditions.

As shown in Fig.12, a series of characteristic distances are selected from 0.002 mm to 0.01mm to estimate the propagation rates. It can be seen that the SCC propagation rate decreases with the propagation of crack, which indicates that the SCC growth rate of small cracks is larger than that of long cracks<sup>[22]</sup>. As represented by Eq.(1), the SCC propagation rate

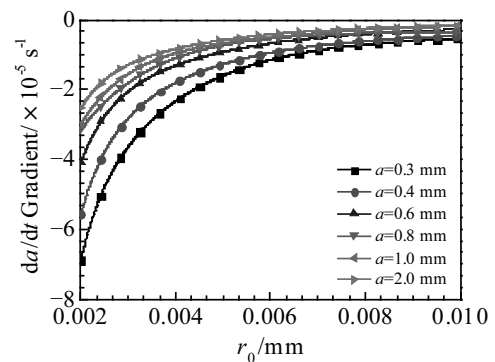


Fig.11 SCC propagation rates gradient in front of crack tip

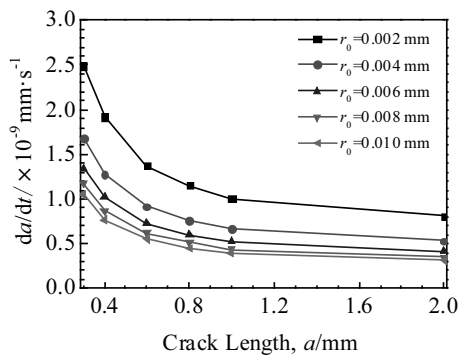


Fig.12 SCC propagation rates calculated at different characteristic distances

depends on the crack tip strain rate. The SCC appears only at an appropriate crack tip strain rate, which may lead to the rupture of crack tip passivation film, combining with the corrosion environment. It is regarded that there is a crack tip strain rate threshold. If the local strain rate at crack tip is greater than the threshold, the small crack will propagate, which will lead to the stress release and strain relaxation at the crack tip, cause a decrease of crack tip strain rate, and result in the decrease of crack propagation rate. With the propagation of crack, the crack tip strain rate decreases. If the crack tip strain rate drops below the threshold, the small crack SCC in the stress corrosion environment can be suppressed.

#### 4 Conclusions

1) It is the strain rather than the stress that controls the initiation and propagation of small cracks. Two methods of dynamic crack propagation and quasi-static crack propagation are proposed to calculate the variation of plastic strain, and the crack tip strain rate can be approximately calculated by the variation of plastic strain at a characteristic distance  $r_0$  in front of a growing small crack tip.

2) The plastic strain variation obtained by quasi-static crack propagation method is slightly larger than that obtained by dynamic crack propagation method, which is determined by the characteristic distance  $r_0$ . The difference between the results calculated by the two methods is not affected by the characteristic distance  $r_0$ .

3) The influence of crack length change on plastic strain variation is small, and the plastic strain variation of crack propagation of small crack is more sensitive than that of the long crack.

4) The effect of characteristic distance on SCC propagation rate is significant for small characteristic distance  $r_0$ , and this effect decreases with the increase of  $r_0$ . The SCC propagation rate of small cracks is larger than that of long cracks. As the

SCC propagation rate is determined by characteristic distance  $r_0$ , it can be suggested that  $r_0$  can be determined by combining experimental SCC data with finite element simulation of the single-edge crack panel specimens under the same environment and material conditions.

#### References

- 1 Wang J A, Kam F B K. *Nuclear Reactor Technology*[J], 1998, 25(S2-3): 117
- 2 Salajka V, Hradil P, Kala J. *Applied Mechanics & Materials*[J], 2013, 284-287: 1247
- 3 Lu Z P, Shoji T, Xue H et al. *Journal of Nuclear Materials*[J], 2012, 423(1-3): 28
- 4 Tang Z M, Hu Shilin, Zhang P Z. *Atomic Energy Science & Technology*[J], 2014, 48(11): 1960
- 5 Fang X R, Xue H, Yang F Q. *Rare Metal Materials and Engineering*[J], 2016, 45(2): 321
- 6 Ford F P. *International Journal of Pressure Vessels & Piping*[J], 1989, 40(5): 343
- 7 Ford F P. *Corrosion*[J], 1996, 52(5): 375
- 8 Gao Y, Kehchih H. *Geochemistry International*[J], 1981, 50(50): 330
- 9 Satoh T, Nakazato T, Moriya S et al. *Journal of Nuclear Materials*[J], 1998, 258-263(4): 2054
- 10 Lumsden J, Mcilree A, Eaker R et al. *Materials Science Forum*[J], 2005, 475-479: 138
- 11 Xue H, Sato Y, Shoji T. *Journal of Pressure Vessel Technology*[J], 2009, 131(2):1
- 12 Fang X R, Xue H, Tang W et al. *ASME 2011 Pressure Vessels & Piping Conference: Code and Standards*[C]. Maryland: ASME, 2011: 1001
- 13 Zhai Z, Toloczko M B, Olszta M J et al. *Corrosion Science*[J], 2017, 123: 76
- 14 Xue H, Ogawa K, Shoji T. *Nuclear Engineering & Design*[J], 2009, 239(4): 628
- 15 Peng Q J, Kwon J, Shoji T. *Journal of Nuclear Materials*[J], 2004, 324(1): 52
- 16 Nowell D, Dragnevski K I, O'Connor S. *International Journal of Fatigue*[J], 2018, 115: 20
- 17 Wang Donghui. *Nuclear Techniques*[J], 2013, 36(4): 1
- 18 Wang Junwei, Zhang Zhouhong, Wu Gaofeng. *Atomic Energy Science and Technology*[J], 2008, 42: 495
- 19 Fuqiang Y, He X, Lingyan Z et al. *Rare Metal Materials & Engineering*[J], 2014, 43(3): 513
- 20 Wang Zhenyu, Zhao Yang, Xu Liang et al. *Advances in Materials Science and Engineering*[J], 2013, 10: 11
- 21 Khor W L, Moore P, Pisarski H et al. *Fatigue & Fracture of Engineering Materials & Structures*[J], 2017, 41(3): 551
- 22 Shi J, Wang J, Macdonald D. *Corrosion Science*[J], 2015, 92: 217

## 核电压力容器 600 合金小裂纹应力腐蚀开裂扩展速率的定量预测

方秀荣, 杨锦辉, 邵艳茹, 欧 雪

(西安科技大学, 陕西 西安 710054)

**摘 要:** 小裂纹应力腐蚀开裂 (SCC) 在核电关键构件 (NPPs) 的全寿命衰减过程有重要影响。通过将薄膜滑移-溶解/氧化模型与弹塑性有限元 (EPFEM) 相结合, 定量预测核电反应堆压力容器 (RPV) 中小裂纹 SCC 扩展速率。根据裂纹尖端力学场的分析, 确定以裂纹尖端应变率来表征小裂纹的萌生和扩展, 并通过距离扩展小裂纹尖端特定的  $r_0$  处的塑性应变 ( $d\epsilon_p/da$ ) 来近似表征裂纹尖端应变率。提出了基于弹塑性断裂力学的动态裂纹扩展和准静态裂纹扩展 2 种方法计算塑性应变 ( $d\epsilon_p/da$ ), 并进行 2 种计算方法比对塑性应变随裂纹长度变化的敏感性, 得到 2 种计算方法之间差异的同时, 也确定小裂纹扩展的塑性应变变化比长裂纹更为敏感。小裂纹的 SCC 扩展速率大于长裂纹的 SCC 扩展速率, 距裂尖的特征距离  $r_0$  是重要的影响因子, 鉴于特定距离  $r_0$  难以确定, 建议通过将相同环境和相同材料下的 SCC 实验数据结合单边拉伸试样的有限元数值计算结果来确定。研究结果能够实现核电关键结构材料的 SCC 扩展速率定量预测及服役压力容器的安全评价。

**关键词:** 600合金; 应力腐蚀裂纹; 定量预测; 裂纹尖端应变; 弹塑性有限元法

---

作者简介: 方秀荣, 女, 1972 年生, 博士, 副教授, 西安科技大学机械工程学院, 陕西 西安 710054, 电话: 029-85583159, E-mail: fangxr098@163.com